Evaluation of Dynamic Relaxation to Solve Kinematics of Concentric Tube Robots

Q. Peyron[1,2], K. Rabenorosoa[2], N. Andreff[2], and P. Renaud[1]

[1] ICUBE-AVR, UDS-CNRS-INSA, Strasbourg, France
[2] FEMTO-ST Institute, Univ. Bourgogne Franche-Comté/CNRS, Besançon, France

Abstract. Concentric tube robots are based on the deformation of elastic pre-curved tubes mounted in a telescopic manner. Their kinematic model consists in a boundary value problem which must be solved during analysis and design. When arbitrary properties and number of the tubes are considered, this model must be solved numerically. We consider in this paper the use of dynamic relaxation to perform this resolution. Its performances in terms of accuracy and computation time are assessed in a case study involving a two-tube CTR. Robustness of the method tuning to variations of CTR behaviour as encountered during a deployment is finally assessed.

Keywords: Concentric tube robot, Continuum robot kinematics, Dynamic relaxation, Boundary value problem

1 Introduction

Concentric tube robots (CTR) consist in telescopic assemblies of pre-curved and elastic tubes, which have been used extensively in minimally invasive surgery [3]. The interactions between the tubes and with their environment create internal wrenches which deform the tubes and place the robot in a certain equilibrium configuration. Acting on the rotation and the translation of the tubes at their base allows a modification in the equilibrium configuration which is used to control the robot tip pose and the backbone shape. The kinematic model of the CTR consists therefore in equilibrium equations issued from continuum mechanics, which must be solved for analysis and design.

As they are composed of elastic beams performing large displacements, CTRs are modelled using either energy considerations [11] or Cosserat rod theory [4]. The equilibrium equations to consider then form a multi-point boundary value problem (BVP), of which the complexity depends on the number and the properties of the tubes and on the considered environment in interaction with the CTR. For a two-tube robot with constant and planar pre-curvature deploying in free space, an analytical solution of the model can be obtained as demonstrated in [4]. When more complex geometries and larger number of tubes are considered, the equilibrium configuration must be computed numerically. Several numerical methods have been used for this purpose that need to handle the presence of boundary conditions at different locations along the CTR backbone. Initial and final boundary conditions are managed independently in a two-step process called the shooting method in [9]. The Galerkin and the LocattoIIIA methods are proposed in [5] and [6] which discretize the CTR along its backbone. The BVP is then transformed into a set of non-linear equations solved with root finding methods. The nodes are placed automatically on the backbone in order to optimize the method accuracy and computation time. Discretization is also considered in [1] where the tubes are represented with a 3D finite element model. Dynamics of the robot are then integrated using a Bathe time integration scheme in order to obtain the CTR equilibrium configuration.

We propose here to consider a discretization of the CTR, but as an initial step to manually control node locations. This allows us to potentially express any boundary condition at a given location, as in the case of contacts with the environment for instance. We show in the following that, after discretization, the problem of solving the CTR kinematics is similar to the one involved in the shape finding of discrete elastic structures such as tensegrity mechanisms [2,8]. The Dynamic Relaxation (DR) method has been successfully used to solve such form-finding problem, and has been already extended to finite element model of rods and plates [10]. We consider therefore in this paper the use of DR to compute the equilibrium configuration of the discrete CTR. This paper is organized as followed. The kinematic model of CTR to be solved is first of all briefly described in Section 2. CTR kinematics in the absence of external load is then considered for sake of simplicity. DR is implemented in Section 3. A first evaluation of the DR performances in terms of accuracy and computation time is finally performed in Section 4, before concluding.

2 Kinematic model of CTR

Evaluation of the DR requires first the derivation of CTR kinematic model. We consider the CTR to be composed of n tubes numbered from the innermost to the outermost. The deployed length and the base angle of tube i are denoted respectively L_i and α_i. The tubes are actuated at the arc-length $s = -\beta_i$, where β_i is the transmission length [5] of tube i. The robot is considered as composed of n sections, the number of tubes being constant along each one. The sections are indexed from the distal end to the proximal one, and the length of the i-th section is denoted ΔL_i.

The local configuration of the robot is defined using a Bishop frame $\mathcal{R}_B$ which z axis is the tangent of the robot backbone. A frame $\mathcal{R}_i$ is attached to each tube i, that is obtained by applying a rotation $(\theta_i(s), \mathbf{z_B})$ to $\mathcal{R}_B$, with $\theta_i(s)$ the twist angle of tube i at arc length s. In the remainder of this paper, we will use when needed subscripts (B and i) to indicate the frame in which vectors are projected.

CTR kinematics are classically described using the curvature of the robot backbone $\boldsymbol{u}(s)$, the pre-curvature vector of each tube i denoted $\hat{\boldsymbol{u}}_{\boldsymbol{i}}(s)$ for tube i and the bending and torsional stiffnesses $k_{ib}(s)$ and $k_{it}(s)$, which form a stiffness matrix $\boldsymbol{K_i}(s)$ such that $\boldsymbol{K_i}(s) = \mathrm{diag}(k_{ib}(s), k_{ib}(s), k_{it}(s))$ [11]. The dependences in s are not mentioned in the following of the paper for sake of compactness. As explained in [11], the equilibrium equations of the robot can be obtained first by expressing the balance of moments at each cross section of the robot:

$$\sum_{i=1}^{m} \boldsymbol{K_j u_B} = \sum_{i=1}^{m} {}^{\boldsymbol{B}}\boldsymbol{R_i K_i}(\boldsymbol{\hat{u}_i} - \hat{u}_{iz}\boldsymbol{e_z}) \tag{1}$$

and second by applying the Euler-Lagrange formula to the total potential energy of the robot, giving:

$$\begin{aligned} & k_{it}\theta_i'' = g_{\theta_i} = k_{it}\hat{u}_{iz}' + k_{it}'(\theta_i' - \hat{u}_{iz}) + \boldsymbol{u_B}^T \frac{\partial^{\boldsymbol{B}}\boldsymbol{R_i}}{\partial \theta_i}\boldsymbol{K_i \hat{u}_i} \\ & i = 1...n \end{aligned} \tag{2}$$

where ${}^{\boldsymbol{B}}\boldsymbol{R_i}$ is the rotation matrix describing the rotation of $\mathcal{R}_i$ with respect to $\mathcal{R}_B$, $[...]'$ is a derivative according to the arc length s and $\boldsymbol{e_z} = \begin{bmatrix}0\ 0\ 1\end{bmatrix}^T$. These differential equations are constrained by boundary conditions modelling the proximal actuation of each tube and the free tube extremities. Assuming that the torsional curvature is constant along the transmission lengths as introduced in [5], these conditions write:

$$\begin{cases} \theta_i(0) = \alpha_i - \beta_i\theta_i'(0) \\ \theta_i'(L_j) = \begin{cases} 0 & , \quad i \neq j \\ \hat{u}_{iz} & , \quad i = j \end{cases} \qquad i = 1...n \end{cases} \tag{3}$$

The kinematic model of the CTR is therefore formulated, in this situation, as a so-called two-point boundary value problem (BVP) composed of the moment balance (1), the energetic equilibrium (2) and the boundary conditions (3).

3 Dynamic relaxation method for CTR

Solving in the general case the CTR kinematic model must be performed numerically. To do this, we discretize first of all the robot geometry in a number N of points along its backbone. The points are placed as denoted for illustration on Figure 1, a point k being located at the arc length s_k. The number of points for section j is designated by N_j so that $N = \sum_{j=1}^{n} N_j$. The twist angles defining the equilibrium configuration of the robot are then evaluated at each point, as illustrated on the figure for point 5 and point $N_3 + 3$. The distance in arc length between point k and point $k+1$ is denoted h_k, so that $h_k = s_{k+1} - s_k$.

The equilibrium equation (2) can then be written using discrete formulation of derivatives. The second-order derivative of $\theta_i(s)$ is replaced by a central second-order finite difference, so that (2) becomes:

$$\begin{aligned} & k_{it,k}\frac{h_k\theta_{i,k-1} - (h_k + h_{k-1})\theta_{i,k} + h_k\theta_{i,k-1}}{h_k h_{k-1}^2} - g_{\theta_i,k} = 0 \\ & \text{with } i = 1...n \quad , \quad k = 2...N-1 \end{aligned} \tag{4}$$

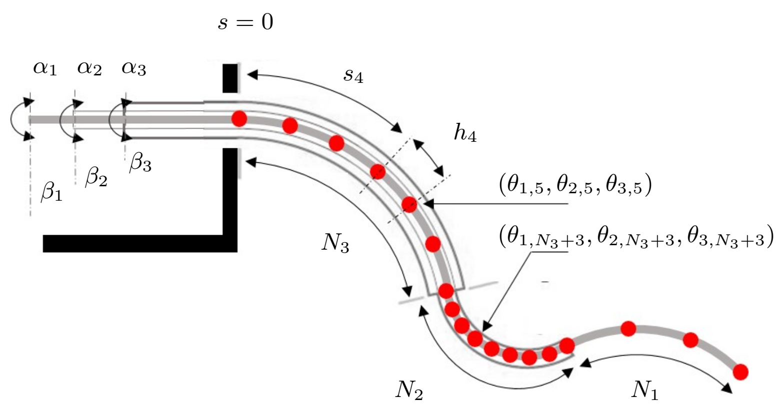

Fig. 1: Representation of the CTR after discretization. Here $n = 3$ and $[N_1 \quad N_2 \quad N_3] = [4 \quad 8 \quad 6]$.

where subscript k denotes an evaluation at point k. The initial and final boundary conditions (3) are then included to the central finite differences evaluated at robot extremities:

$$
\begin{aligned}
&\frac{\beta_i\theta_{i,2} - (\beta_i + h_1)\theta_{i,1} + h_1\alpha_i}{h_1\beta_i^2} - g_{\theta_i,1} = 0 \\
&\frac{\theta_{i,Nf} - 2\theta_{i,N} + \theta_{i,N-1}}{h_N^2} - g_{\theta_i,N} = 0 \\
&\theta_{i,Nf} = \hat{u}_{iz,N}h_N + \theta_{i,N} \\
&i = 1...n
\end{aligned}
\tag{5}
$$

Gathering the twist angle in a state vector $\boldsymbol{X}$ such that:

$$
\boldsymbol{X} = \left[\theta_{1,1} \; ... \; \theta_{1,N} \; \theta_{2,1} \; ... \; \theta_{n,N}\right]^T, \tag{6}
$$

the boundary-value problem is thus transformed into a set of non-linear equations of the form:

$$
\boldsymbol{G}(\boldsymbol{X}) = \boldsymbol{0} \tag{7}
$$

The resulting discrete model is similar to the ones involved in discrete elastic structures, and can be solved using DR. With DR, state variables are artificially considered as function of time. The principle is to initially place the robot in an arbitrary shape, which means an initial value of $\boldsymbol{X}$ is guessed. The CTR is then relaxed virtually until it reaches an equilibrium. The dynamics of the state variables according to the virtual time are imposed to fit a second order damped differential equation:

$$
\boldsymbol{M}\ddot{\boldsymbol{X}} + \boldsymbol{D}\dot{\boldsymbol{X}} + \boldsymbol{G}(\boldsymbol{X}) = \boldsymbol{0} \tag{8}
$$

where $\boldsymbol{M}$ and $\boldsymbol{D}$ are called the fictitious mass matrix and damping matrix respectively, and are usually diagonal matrices [10]. The equilibrium configuration resulting from the DR is then the steady state of (8). The computational efficiency of DR, in terms of numerical stability and computation time relies in the selection of diagonal elements of $\boldsymbol{M}$ and $\boldsymbol{D}$ [10].

The mass matrix $\boldsymbol{M}$ is classically determined in order to maximize integration time-step while ensuring numerical stability, which includes integration stability and convergence of the dynamical system. We consider the integration with the `ode45` solver of Matlab (The MathWorks Inc., Natick, USA) which processes a 4-th order Runge-Kutta method. This implicit integration scheme automatically optimizes the integration time step. Consequently, following the same arguments as [12], the modulus of the mass matrix coefficients do not need to be tuned and can be chosen as unitary. Their sign must be chosen equal to the diagonal components of the gradient of $\boldsymbol{G}$ [2]. According to [10], the damping coefficients are determined to minimize the virtual time at which the steady state is reached. Since this virtual time affects the DR performances, the question of their selection is considered in the following.

4 Method evaluation

A realistic case study is chosen for the method evaluation using the CTR geometry given in [7] and described by the parameters gathered in Table 1.

4.1 Initial validation of the DR

Obviously, DR is of interest only if it can allow us to solve accurately the CTR kinematic model. Given the numerical values of $\boldsymbol{G}$ components, the diagonal components of $\boldsymbol{M}$ and $\boldsymbol{D}$ are in an initial step chosen equal to -1 and -10 respectively. The dynamical system is then integrated using `ode45` on a virtual time interval large enough to reach the steady state. The time interval is determined by trials and errors process in the following. The initial guess is chosen as $\theta_{i,k} = a_i, \forall k$ for tube i.

Since the accuracy of the discrete derivatives involved in (4) depends on the number of discretization points N_1 and N_2, so does the accuracy of the computed equilibrium. With $[N_1, N_2] = [4, 100]$ and the steady state defined by a threshold on $\|\boldsymbol{G(X)}\|$ equal to 1.10^{-6}, that we will keep in the following of the paper, the equilibrium configuration is reached within a virtual time interval of 1.10^{6}s. Comparing the DR results with the analytical solution of two-tube CTR fully overlapped provided in [4], the maximum relative error is of approximately 0.5%, validating thus the ability of the DR to compute accurate CTR equilibria.

4.2 Adjustement of DR parameters

Selection of the damping coefficients in DR is important to control the steady step computation time [10]. The main approach to determine them consists in linearizing (8) and to identify each of its equations to a standard second order

	Tube 1	Tube 2
α_i (rad)	$\pi/4$	0
L_i (mm)	117	100
β_i (mm)	0	0
$\hat{u}_{ix}(\text{mm}^{-1})$	1/60	1/60
k_{ib} (N.mm^2)	1	1
k_{it} (N.mm^2)	1/1.3	1/1.3

Table 1: Geometrical and mechanical properties of the two tubes.

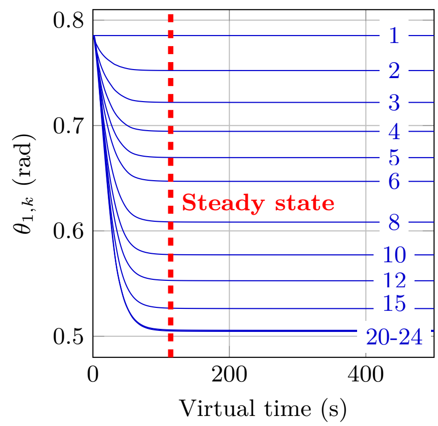

Fig. 2: Evaluation of torsion angles of tube 1 using DR. Index k on the curve.

differential equation with damping factor ξ and corner pulsation ω_0. The optimal damping corresponds then to $\xi = 1$, and writes for equations numbered k:

$$D_k = 2\omega_{0,k} M_k \tag{9}$$

Different methods exist in the literature to calculate ω_0. In [12], (8) is integrated once without damping. This results in an oscillating response which fundamental pulsation is measured and used as corner pulsation in (9). This method has been proved to provide efficient damping matrices in several application cases of structural mechanics [12] and is consequently chosen here.

The optimal damping matrix is determined for the two-tube CTR described before with $[N_1, N_2] = [4, 20]$, which ensures acceptable accuracy of 2% and reasonable computation times. The dynamical system is integrated without damping on a virtual time interval of 2000s so that several oscillations are generated to identify ω_0. Using the damping matrix obtained with (9), Figure 2 is generated by applying DR. The torsion angles converge at the virtual time 114s, to compare with 9500s considering the arbitrary values used in section 4.1. Such virtual time is obtained after approximately 5s of simulation on an Intel Core I5-6300HQ CPU running at 2.3GHz.

4.3 Robustness of the DR parameter selection

It would be interesting to be able to compute several equilibrium configurations of CTR with the same mass and damping matrices in order to simplify the use of DR during the kinematic analysis of a CTR. This would be particularly interesting for the simulation of CTR deployments, where several equilibria must be computed for consecutive values of the actuation inputs.

The mass and damping coefficients determined in the previous section are here used to solve the CTR kinematic model for several values of the angle α_1

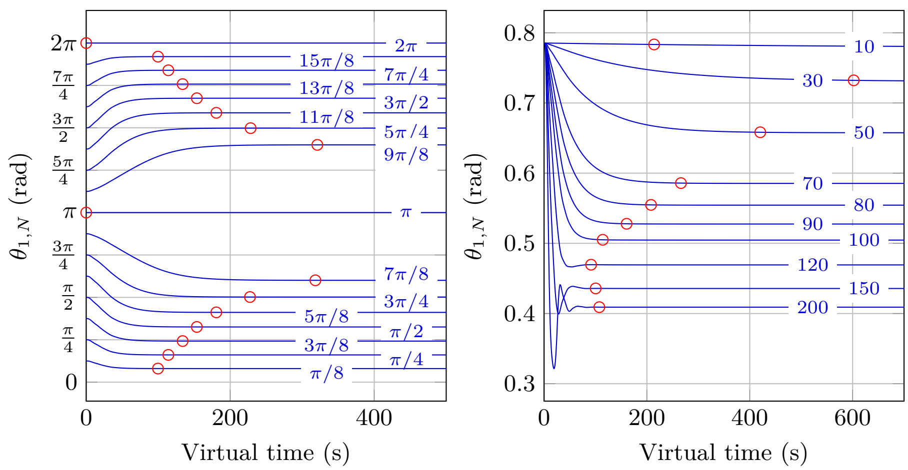

(a) Variations of α_1 (rad).

(b) Variations of L_2 (mm).

Fig. 3: Evolution of the virtual time responses obtained with DR for several values of actuation parameters. Steady state times localized with a red circle on each curve. Parameter values written on the curves.

and of the deployed length L_2 with DR. The Figure 3a shows that the method, starting from the initial guess proposed previously, is able to solve the CTR kinematics for all values of α_1, even for the unstable configuration where the tubes are placed in opposition [7]. The virtual time at which the equilibrium is reached equals 321s for $\alpha_1 = \pi \pm \pi/8$ and 114s for $\alpha_1 = \pm\pi/8$, indicating an increase in computation time in the neighbourhood of the unstable configuration. The Figure 3b shows the ability to solve the CTR kinematics for all values of L_2 at the cost of increased virtual response time, which are reached however with acceptable computation time of maximum 13s for $L_2 = 30$.

5 Conclusion

In this paper we have proposed to use dynamic relaxation to solve kinematic model of CTR. From our case study, it appears first that the numerical method is able to compute accurately equilibrium configurations of CTR. Second, computation time can be minimized dramatically by choosing an appropriate damping matrix to reach acceptable values even when CTR geometry is modified during a deployment.

Such initial encouraging results open several perspectives. On one hand, more efficient integration methods in term of computation time could be used to reach the steady-state, such as the explicit integration schemes. On the other hand the efficiency of the damping may be improved by applying tuning methods all along the integration, as proposed in [13]. This could largely improve DR efficiency.

Further use to solve CTR kinematics in complex situations with interactions will then be evaluated.

Acknowledgement

This work was supported by the French National Agency for Research within the Biomedical Innovation program (NEMRO ANR-14-CE17-0013), the Investissements d'Avenir (Robotex ANR-10-EQPX-44, Labex CAMI ANR-11-LABX-0004 and Labex ACTION ANR-11-LABX-0001-01) and Aviesan France Life Imaging infrastructure.

References

1. C. Baek, K. Yoon, and D. Kim. Finite element modeling of concentric-tube continuum robots. *Structural Engineering and Mechanics*, 57(5):809–821, March 2016.
2. Michael R. Barnes. Form Finding and Analysis of Tension Structures by Dynamic Relaxation. *International Journal of Space Structures*, 14(2):89–104, June 1999.
3. J. Burgner-Kahrs, D. C. Rucker, and H. Choset. Continuum Robots for Medical Applications: A Survey. *IEEE Transactions on Robotics*, 31(6):1261–1280, December 2015.
4. P. E. Dupont, J. Lock, B. Itkowitz, and E. Butler. Design and Control of Concentric-Tube Robots. *IEEE Transactions on Robotics*, 26(2):209–225, April 2010.
5. H. B. Gilbert, J. Neimat, and R. J. Webster. Concentric Tube Robots as Steerable Needles: Achieving Follow-the-Leader Deployment. *IEEE Transactions on Robotics*, 31(2):246–258, April 2015.
6. C. Girerd, K. Rabenorosoa, and P. Renaud. Combining Tube Design and Simple Kinematic Strategy for Follow-the-Leader Deployment of Concentric Tube Robots. In *Advances in Robot Kinematics 2016*, Springer Proceedings in Advanced Robotics, pages 23–31. Springer, Cham, 2018. DOI: 10.1007/978-3-319-56802-7_3.
7. J. Ha, F. C. Park, and P. E. Dupont. Elastic Stability of Concentric Tube Robots Subject to External Loads. *IEEE Transactions on Biomedical Engineering*, 63(6):1116–1128, June 2016.
8. W. J. Lewis, M. S. Jones, and K. R. Rushton. Dynamic relaxation analysis of the non-linear static response of pretensioned cable roofs. *Computers & Structures*, 18(6):989–997, January 1984.
9. J. Lock, G. Laing, M. Mahvash, and P. E. Dupont. Quasistatic modeling of concentric tube robots with external loads. In *2010 IEEE/RSJ International Conference on Intelligent Robots and Systems (IROS)*, pages 2325–2332, October 2010.
10. M. Rezaiee-Pajand and J. Alamatian. The dynamic relaxation method using new formulation for fictitious mass and damping. *Structural Engineering and Mechanics*, 34(1):109–133, 2010.
11. D. C. Rucker, R. J. Webster, G. S. Chirikjian, and N. J. Cowan. Equilibrium Conformations of Concentric-tube Continuum Robots. *The International Journal of Robotics Research*, 29(10):1263–1280, September 2010.
12. K R Rushton. Dynamic-relaxation solutions of elastic-plate problems. *Journal of Strain Analysis*, 3(1):23–32, January 1968.
13. L. C. Zhang, M. Kadkhodayan, and Y. W. Mai. Development of the maDR method. *Computers & Structures*, 52(1):1–8, July 1994.